

## Original Article

# Value of intravoxel incoherent motion diffusion-weighted imaging in differentiating the pathological grade of clear cell renal cell carcinoma

Xiaoping Yu<sup>1</sup>, Yuhui Qin<sup>1</sup>, Yan Liu<sup>1</sup>, Congrui Li<sup>1</sup>, Yu Xie<sup>2</sup>, Yan Sun<sup>1</sup>

Departments of <sup>1</sup>Diagnostic Radiology, <sup>2</sup>Urological Surgery, Hunan Cancer Hospital and The Affiliated Cancer Hospital of Xiangya School of Medicine, Central South University, Changsha, Hunan, PR China

Received August 27, 2017; Accepted July 2, 2018; Epub October 15, 2018; Published October 30, 2018

**Abstract:** We explored the value of intravoxel incoherent motion diffusion-weighted imaging (IVIM-DWI) in differentiating the pathological grades of clear cell renal cell carcinoma (ccRCC). Preoperative IVIM-DWI data from 42 patients with ccRCC were prospectively analyzed. IVIM-DWI parameters (apparent diffusion coefficient [ADC], pure diffusion coefficient [D], pseudo-diffusion coefficient [D\*] and perfusion fraction [f]) were compared between the low Fuhrman grade (grades I and II) and high Fuhrman grade (grades III and IV) ccRCC groups. The high-grade ccRCC group exhibited significantly lower ADC ( $[1.10 \pm 0.58] \times 10^{-3} \text{ mm}^2/\text{s}$  vs.  $[1.62 \pm 0.24] \times 10^{-3} \text{ mm}^2/\text{s}$ ,  $P = 0.003$ ), D ( $[1.40 \pm 0.20] \times 10^{-3} \text{ mm}^2/\text{s}$  vs.  $[1.73 \pm 0.18] \times 10^{-3} \text{ mm}^2/\text{s}$ ,  $P < 0.001$ ) and f ( $0.15 \pm 0.09$  vs.  $0.27 \pm 0.08$ ,  $P < 0.001$ ) values compared with the low-grade group. There was no significant difference in the D\* values between the two groups ( $[72.18 \pm 90.28] \times 10^{-3} \text{ mm}^2/\text{s}$  vs.  $[109.46 \pm 129.07] \times 10^{-3} \text{ mm}^2/\text{s}$ ,  $P = 0.772$ ). The optimal cut-off values (area under the curve, sensitivity and specificity) for distinguishing low- and high-grade ccRCCs were as follows: ADC =  $1.14 \times 10^{-3} \text{ mm}^2/\text{s}$  (0.768, 95.2% and 66.7%), D =  $1.64 \times 10^{-3} \text{ mm}^2/\text{s}$  (0.931, 81.0% and 100.0%), and f = 0.18 (0.829, 85.7% and 66.7%). IVIM-DWI may be helpful in differentiating the Fuhrman grades of ccRCC.

**Keywords:** Intravoxel incoherent motion, diffusion-weighted imaging, renal carcinoma, Fuhrman grade, sensitivity and specificity

## Introduction

Comprising approximately 80%-85% of all renal cell carcinomas (RCCs) [1, 2], clear cell RCC (ccRCC) is usually associated with a poorer prognosis than the other subtypes of RCCs [3, 4]. Preoperatively obtaining an accurate pathological ccRCC grade is helpful for optimizing surgical approaches and predicting the patient's prognosis [5].

Previous studies on ccRCC have explored that traditional diffusion-weighted imaging (DWI) is helpful for identifying the Fuhrman pathological grade of tumors [6-11], which is widely used for ccRCC in current clinical practice [12, 13]. However, conflicting observations were reported across prior investigations [6-11]. This might be due to the shortcoming of ADC in characterizing the diffusion motion of water molecules since ADC cannot separate the motion caused by the Brownian movement from that caused by microcirculatory perfusion, which might neg-

atively influence the performance of ADC on differentiating the pathological grade of ccRCC.

With the ability to simultaneously quantitate the two kinds of diffusion motion in tissues, intravoxel incoherent motion DWI (IVIM-DWI) has become increasingly utilized in preoperatively grading a variety of tumors [14-17]. Nevertheless, the performance of IVIM-DWI on evaluating the Fuhrman grade of ccRCC has remained unclear. Thus, this study aimed to investigate the utility of IVIM-DWI in differentiating low- and high-grade ccRCCs.

## Materials and methods

### Subjects

This single-center, prospective study was approved by the Medical Ethics Committee of our institution and conducted in accordance with the Declaration of Helsinki. From May 2015 to February 2017, 59 consecutive patients who

## Differentiation degrees of kidney cancer

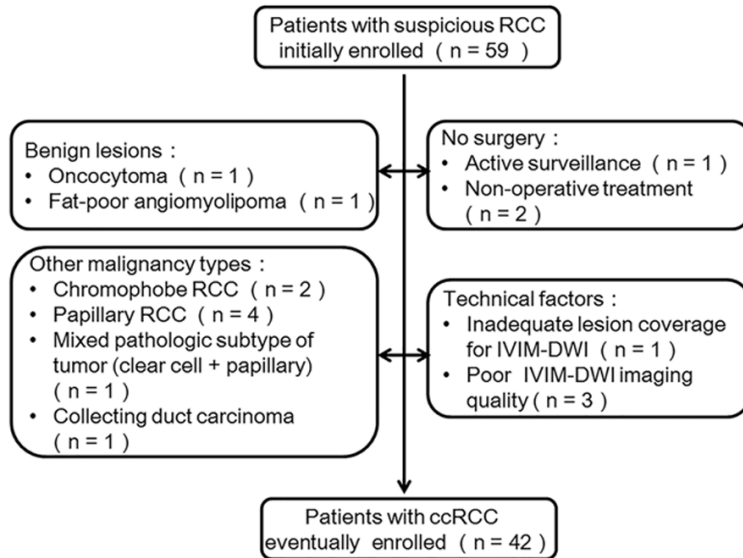


**Figure 1.** Flow diagram of patient elimination.

**Table 1.** Characteristics of patients and tumors

Parameter	Low-grade (n = 21)	High-grade (n = 21)	P value
Age (years)	55.38 ± 9.06	59.14 ± 8.99	0.186
Long diameter (mm)	53.33 ± 15.52	49.48 ± 14.95	0.385
Gender			0.743
Male	6	8	
Female	15	13	
Location			0.758
Right kidney	11	9	
Left kidney	10	12	

**Table 2.** Comparisons of IVIM-DWI parametric values (mean ± standard deviation) between the low- and high-grade ccRCC groups

Parameter	Low-grade (n = 21)	High-grade (n = 21)	P value
ADC ( $\times 10^{-3}$ mm <sup>2</sup> /s)	1.62 ± 0.24	1.10 ± 0.58	0.003
D ( $\times 10^{-3}$ mm <sup>2</sup> /s)	1.73 ± 0.18	1.40 ± 0.20	0.000
D* ( $\times 10^{-3}$ mm <sup>2</sup> /s)	72.18 ± 90.28	109.46 ± 129.07	0.772
f	0.27 ± 0.08	0.15 ± 0.09	0.000

IVIM-DWI, intravoxel incoherent motion diffusion-weighted imaging; ccRCC, clear cell renal cell carcinoma; ADC, apparent diffusion coefficient; D, pure diffusion coefficient; D\*, pseudo-diffusion coefficient; f, perfusion fraction.

underwent preoperative magnetic resonance imaging (MRI) for the evaluation of renal masses at our institution were initially enrolled. The inclusion criteria were (1) new suspicious RCC detected by conventional CT and/or MRI with a lesion diameter larger than 10 mm; (2) scheduled for surgical resection; (3) lacking prior anti-tumor therapy; and (4) older than 18 years of

age. Patients were excluded if they (1) received a biopsy on a renal lesion within the past month; (2) had MRI contraindication; or (3) did not sign the informed consent form. After initial enrollment, preoperative MRI was performed, with a mean time interval between the MRI and subsequent surgical resection of 6 days (range, 4-9 days). Seventeen patients were eliminated from this study because of technical factors (n = 4), lack of surgical resection (n = 3), or undesired final histopathological results (n = 10). These eliminations are summarized in **Figure 1**. Thus, the present study ultimately included 42 patients with ccRCC, which were all classified as solitary lesions. The numbers of ccRCC with Fuhrman nuclear grades I, II, III and IV were 9, 12, 16 and 5, respectively. Patients with Fuhrman grade I or II were classified into the low-grade group of the present study, while those with grade III or IV were divided into the high-grade group. Thus, both the low- and high-grade ccRCC groups comprised 21 tumors. The characteristics of the ccRCC patients and tumors are presented in **Table 1**.

### MRI protocols

All MRI examinations were performed with the patients in the supine position on a 1.5-Tesla clinical MRI scanner (Optima MR360, GE Healthcare, Waukesha, WI, USA) using an 8-channel body phased-array coil. The patients were trained to breathe deeply prior to holding their breath, and their abdominal wall was secured in front of the coil by using a bandage to reduce motion artifacts during MRI data acquisition.

The conventional MRI protocols included the following sequences: 1) axial T1-weighted dual-

## Differentiation degrees of kidney cancer

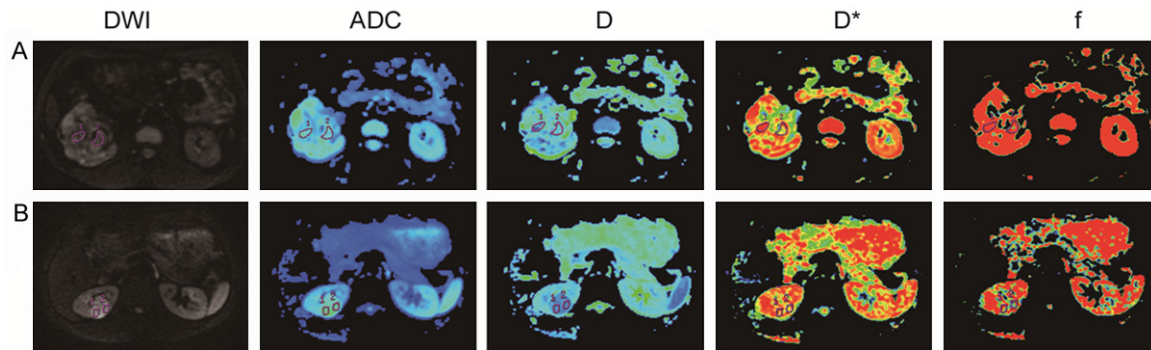


**Figure 2.** The images in row (A) are the ADC, D, D\*, and  $f$  maps of a clear cell renal cell carcinoma (Fuhrman grade II) in the left kidney of a 67-year-old man from the low-grade group. The ADC, D, D\* and  $f$  values were  $2.03 \times 10^{-3}$  mm<sup>2</sup>/s,  $1.75 \times 10^{-3}$  mm<sup>2</sup>/s,  $65 \times 10^{-3}$  mm<sup>2</sup>/s and 0.29, respectively. The images in row (B) correspond to the IVIM-DWI parametric maps of a clear cell renal cell carcinoma (Fuhrman grade III) in the right kidney of a 51-year-old man from the high-grade group. The ADC, D, D\* and  $f$  values were  $1.13 \times 10^{-3}$  mm<sup>2</sup>/s,  $1.42 \times 10^{-3}$  mm<sup>2</sup>/s,  $79 \times 10^{-3}$  mm<sup>2</sup>/s and 0.17, respectively.

echo in-phase and out-of-phase sequences: (number of slices, 24; time of repetition [TR], 205 ms; time of echo [TE], 2.1/4.2 ms; slice thickness, 4 mm; slice space, 1 mm; field of view [FOV], 380 × 342 mm; acquisition matrix, 256 × 160; number of excitations [NEX], 1); 2) axial T2-weighted fast spin-echo (FSE) images with fat suppression (number of slices, 24; TR, 6000 ms; TE, 86.4 ms; slice thickness, 4 mm; slice space, 1 mm; FOV, 380 × 342 mm; acquisition matrix, 320 × 192; number NEX, 2); and 3) axial and coronal T1-weighted fast spoiled gradient echo (FSPGR) contrast-enhanced images with fat suppression (number of slices, 24; TR, 165 ms; TE, 2.3 ms; slice thickness, 4 mm; slice space, 1 mm; FOV, 400 × 400 mm; acquisition matrix, 384 × 192; number NEX, 2). The contrast agent gadodiamide (Omniscan®, GE Healthcare) was administered intravenously at a dose of 0.1 mmol/kg of body weight.

IVIM-DWI was performed before the administration of gadodiamide. Twelve  $b$  values (0, 20, 30, 50, 80, 100, 150, 200, 400, 600, 800 and 1000 s/mm<sup>2</sup>) were applied with a single-shot diffusion-weighted spin-echo echo-planar sequence. The lookup table of gradient direction was modified to allow multiple  $b$ -value measurements in one series. Parallel imaging was used with an acceleration factor of 2. In total, 20 axial slices covering the kidney region were obtained with an FOV of 380 × 304 mm, a slice thickness of 4 mm, a slice gap of 1 mm, a TR of 6000 ms, a TE of 81.7 ms, a matrix of 128 × 130, and an NEX of 4.

### IVIM-DWI analysis

All IVIM-DWI data were imported into the Advantage Workstation with FuncTool software (version AW 4.6, GE Healthcare) for post-processing. The IVIM-DWI data were independently and double-blindly evaluated by two radiologists (L.Y. and Y.X., with 20 and 15 years of experience in abdomen radiology, respectively), using the MADC software kit. The main principle and procedures of the IVIM-DWI analysis were described previously [18, 19]. Briefly, the D, D\* and  $f$  values was derived from the formula  $S_b/S_0 = (1-f) \exp(-b D) + f \exp(-b D^*)$ , where  $S_b$  is the signal intensity with diffusion gradient  $b$  ( $b \neq 0$  s/mm<sup>2</sup>),  $S_0$  is the signal intensity for the  $b$  value of 0 s/mm<sup>2</sup>, D is the true diffusion coefficient indicating the pure diffusion of water molecules, D\* is the pseudo-diffusion coefficient demonstrating microcirculation perfusion, and  $f$  is the microvascular volume fraction representing the fraction of diffusion related to microcirculation perfusion. The ADC value was generated from the formula  $S_b/S_0 = \exp(-b \text{ADC})$  based on conventional DWI with MRI data at high  $b$  values (200, 400, 600, 800 and 1000 s/mm<sup>2</sup>).

The regions of interest (ROIs) were manually drawn in the tumor parenchyma. Six ROIs were manually drawn by each observer for each tumor on its DWI images ( $b = 800$  s/mm<sup>2</sup>) of at least 3 sections using conventional axial T1-weighted, T2-weighted and contrast-enhanced images as references. Care was taken to avoid the inclusion of visual cystic change,

**Table 3.** Diagnostic performance of IVIM-DWI parameters for differentiating high- and low-grade ccRCCs

Parameter	Cut-off value	AUC (95% CI)	Sensitivity	Specificity
ADC	$1.14 \times 10^{-3} \text{ mm}^2/\text{s}$	0.768 (0.604-0.931)	95.2%	66.7%
D	$1.64 \times 10^{-3} \text{ mm}^2/\text{s}$	0.931 (0.849-1.000)	81.0%	100.0%
<i>f</i>	0.18	0.829 (0.705-0.953)	85.7%	66.7%

IVIM-DWI, intravoxel incoherent motion diffusion-weighted imaging; ccRCC, clear cell renal cell carcinoma; ADC, apparent diffusion coefficient; D, pure diffusion coefficient; D\*, pseudo-diffusion coefficient; *f*, perfusion fraction; AUC, area under curve; CI, confidence interval.

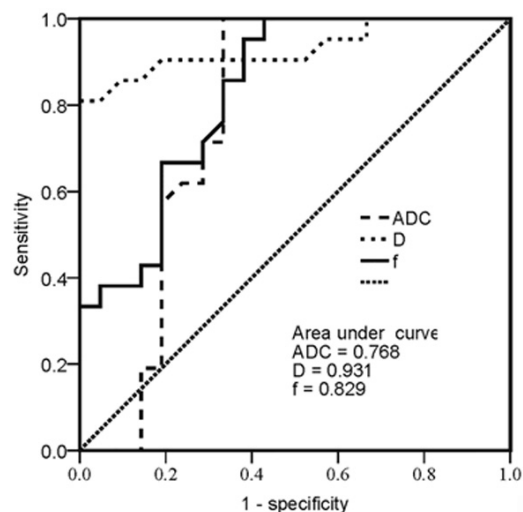


**Figure 3.** Receiver operating characteristic curves of ADC, D and *f* in discriminating between the high- and low-grade ccRCC groups.

necrosis, hemorrhage, large vessel and fat areas. The ROIs were subsequently propagated to the IVIM-DWI parametric maps for measuring the metric values. For each parameter, 12 numerical values were generated for each lesion by the two observers. The final value for each parameter was designated the mean value of the 12 numerical values above.

*Pathological grading*

The pathological grade of ccRCC from the resected specimen was determined by a veteran uropathologist with 12 years of specialty experience according to the Fuhrman grading system [20, 21].

*Statistical analysis*

Intra-class correlation coefficients were calculated to evaluate inter-observer variability. The IVIM-DWI parametric values for the low- and

high-grade ccRCC groups were expressed as the mean ± standard deviation and analyzed using SPSS v22.0 (IBM Corporation, Armonk, NY, USA) and MedCalc v15.0 (MedCalc Software bvba, Ostend, Belgium). *P* values less than 0.05 were considered statistically significant. Chi-squared tests were performed to test differences in the patients' gender and tumor locations between the low- and high-grade groups. Non-parametric Mann-Whitney U tests were used to compare differences in the IVIM-DWI metric values, lesion sizes and patients' ages between the two groups. Receiver operating characteristic (ROC) curves were generated for the IVIM-DWI parameters with statistically significant differences to determine their optimal cut-off values resulting in the best possible diagnostic accuracy according to the Youden Index.

Results

**Results**

The intra-class correlation coefficients (95% CI) of inter-observer reproducibility for the measurements of ADC, D, D\* and *f* were 0.873 (0.765-0.932), 0.930 (0.870-0.962), 0.814 (0.655-0.900) and 0.894 (0.803-0.943), respectively, which demonstrates optimal inter-observer reproducibility and consistency.

The IVIM-DWI parametric values for the two ccRCC groups are summarized in **Table 2**. The high-grade group exhibited significantly lower ADC, D and *f* values than the low-grade group (all *P*<0.01). **Figure 2** shows representative images of low- and high-grade ccRCCs. For differentiating low- and high-grade ccRCCs based on ROC curve analysis, the area under the curve (AUC) value for D was the highest (0.931), followed by that for *f*, whereas ADC had the lowest AUC value (**Table 3** and **Figure 3**).

**Discussion**

The present study demonstrated that both the diffusion- and perfusion-related IVIM-DWI parameters exhibited the potential to discriminate the pathological Fuhrman grade of ccRCC. Moreover, the microcirculatory perfusion might negatively influence the performance of diffu-

## Differentiation degrees of kidney cancer

sion on distinguishing ccRCC lesions with different pathological grades.

High-grade ccRCC showed obviously lower ADC,  $D$  and  $f$  values than low-grade ccRCC in the current study. This was consistent with previous findings on DWI [8, 9], which suggests that the diffusion movement of water molecules is more restricted in high-grade ccRCC than in low-grade ccRCC, since both ADC and  $D$  are diffusion-related parameters [18]. Our observation was also similar to previous studies in which ccRCC with low Fuhrman grade demonstrated higher enhancement degree on MRI than high-grade tumor [22, 23], which indicates that high-grade ccRCC might own lower vascularization than low-grade ccRCC, as parameter  $f$  depends mainly on the microvessel density of tissues [24, 25].

In our study, the pure perfusion parameter ( $D^*$ ) value did not show a significant difference between the two ccRCC groups, which was in line with prior findings on other malignancies [15-17]. This might result from the poor reproducibility in the measurement of  $D^*$  [26-28]. Additionally, the pure perfusion parameter ( $D$ ) performed better than the perfusion-related metrics (ADC and  $f$ ) in the differentiation between the high- and low-grade ccRCCs in this study. Taken together, it may be inferred that microcirculatory perfusion would have a negative impact on the diagnostic efficiency of diffusion in discriminating ccRCC lesions with different Fuhrman grades.

In conclusion, our observations demonstrated that IVIM-DWI, especially its pure diffusion parameter  $D$ , may be helpful in differentiating the Fuhrman grades of ccRCC.

### Acknowledgements

This study was supported by funding from the Provincial Health and Family Planning Commission, Hunan, PR China (contract grant number: B2014-115), and the Provincial Key Clinical Specialty (Medical Imaging) Development Program from the Health and Family Planning Commission of Hunan Province (contract grant number: 2015/43).

### Disclosure of conflict of interest

None.

**Address correspondence to:** Xiaoping Yu and Yan Liu, Department of Diagnostic Radiology, Hunan Cancer Hospital, The Affiliated Cancer Hospital of Xiangya School of Medicine, Central South University, No. 283 Tongzipo Road, Changsha 410013, Hunan, PR China. Tel: 0086-731-89762577; Fax: 0086-731-89762577; E-mail: yuxiaoping@hnszlyy.com (XPY); Tel: 0086-731-89762576; Fax: 0086-731-89762577; E-mail: liuyan@hnszlyy.com (YL)

### References

- [1] Jemal A, Siegel R, Ward E, Hao Y, Xu J and Thun MJ. Cancer statistics, 2009. *CA Cancer J Clin* 2009; 59: 225-249.
- [2] Chow WH, Dong LM and Devesa SS. Epidemiology and risk factors for kidney cancer. *Nat Rev Urol* 2010; 7: 245-257.
- [3] Delahunt B, Bethwaite PB and Nacey JN. Outcome prediction for renal cell carcinoma: evaluation of prognostic factors for tumours divided according to histological subtype. *Pathology* 2007; 39: 459-465.
- [4] Gudbjartsson T, Hardarson S, Petursdottir V, Thoroddsen A, Magnusson J and Einarsson GV. Histological subtyping and nuclear grading of renal cell carcinoma and their implications for survival: a retrospective nation-wide study of 629 patients. *Eur Urol* 2005; 48: 593-600.
- [5] Ghavamian R, Chevillat JC, Lohse CM, Weaver AL, Zincke H and Blute ML. Renal cell carcinoma in the solitary kidney: an analysis of complications and outcome after nephron sparing surgery. *J Urol* 2002; 168: 454-459.
- [6] Goyal A, Sharma R, Bhalla AS, Gamanagatti S, Seth A, Iyer VK and Das P. Diffusion-weighted MRI in renal cell carcinoma: a surrogate marker for predicting nuclear grade and histological subtype. *Acta Radiol* 2012; 53: 349-358.
- [7] Yu X, Lin M, Ouyang H, Zhou C and Zhang H. Application of ADC measurement in characterization of renal cell carcinomas with different pathological types and grades by 3.0T diffusion-weighted MRI. *Eur J Radiol* 2012; 81: 3061-3066.
- [8] Maruyama M, Yoshizako T, Uchida K, Araki H, Tamaki Y, Ishikawa N, Shiina H and Kitagaki H. Comparison of utility of tumor size and apparent diffusion coefficient for differentiation of low- and high-grade clear-cell renal cell carcinoma. *Acta Radiol* 2015; 56: 250-256.
- [9] Rosenkrantz AB, Niver BE, Fitzgerald EF, Babb JS, Chandarana H and Melamed J. Utility of the apparent diffusion coefficient for distinguishing clear cell renal cell carcinoma of low and high nuclear grade. *AJR Am J Roentgenol* 2010; 195: W344-351.

## Differentiation degrees of kidney cancer

- [10] Abdel Razek AA and Kamal E. Nasopharyngeal carcinoma: correlation of apparent diffusion coefficient value with prognostic parameters. *Radiol Med* 2013; 118: 534-539.
- [11] Sandrasegaran K, Sundaram CP, Ramaswamy R, Akisik FM, Rydberg MP, Lin C and Aisen AM. Usefulness of diffusion-weighted imaging in the evaluation of renal masses. *AJR Am J Roentgenol* 2010; 194: 438-445.
- [12] Minardi D, Lucarini G, Mazzucchelli R, Milanese G, Natali D, Galosi AB, Montironi R, Biagini G and Muzzonigro G. Prognostic role of Fuhrman grade and vascular endothelial growth factor in pT1a clear cell carcinoma in partial nephrectomy specimens. *J Urol* 2005; 174: 1208-1212.
- [13] Hong SK, Jeong CW, Park JH, Kim HS, Kwak C, Choe G, Kim HH and Lee SE. Application of simplified fuhrman grading system in clear-cell renal cell carcinoma. *BJU Int* 2011; 107: 409-415.
- [14] Hu YC, Yan LF, Wu L, Du P, Chen BY, Wang L, Wang SM, Han Y, Tian Q, Yu Y, Xu TY, Wang W and Cui GB. Intravoxel incoherent motion diffusion-weighted MR imaging of gliomas: efficacy in preoperative grading. *Sci Rep* 2014; 4: 7208.
- [15] Togao O, Hiwatashi A, Yamashita K, Kikuchi K, Mizoguchi M, Yoshimoto K, Suzuki SO, Iwaki T, Obara M, Van Cauteren M and Honda H. Differentiation of high-grade and low-grade diffuse gliomas by intravoxel incoherent motion MR imaging. *Neuro Oncol* 2016; 18: 132-141.
- [16] Woo S, Lee JM, Yoon JH, Joo I, Han JK and Choi BI. Intravoxel incoherent motion diffusion-weighted MR imaging of hepatocellular carcinoma: correlation with enhancement degree and histologic grade. *Radiology* 2014; 270: 758-767.
- [17] Zhang YD, Wang Q, Wu CJ, Wang XN, Zhang J, Liu H, Liu XS and Shi HB. The histogram analysis of diffusion-weighted intravoxel incoherent motion (IVIM) imaging for differentiating the gleason grade of prostate cancer. *Eur Radiol* 2015; 25: 994-1004.
- [18] Le Bihan D, Breton E, Lallemand D, Aubin ML, Vignaud J and Laval-Jeantet M. Separation of diffusion and perfusion in intravoxel incoherent motion MR imaging. *Radiology* 1988; 168: 497-505.
- [19] Xiao-ping Y, Jing H, Fei-ping L, Yin H, Qiang L, Lanlan W and Wei W. Intravoxel incoherent motion MRI for predicting early response to induction chemotherapy and chemoradiotherapy in patients with nasopharyngeal carcinoma. *J Magn Reson Imaging* 2016; 43: 1179-1190.
- [20] Fuhrman SA, Lasky LC and Limas C. Prognostic significance of morphologic parameters in renal cell carcinoma. *Am J Surg Pathol* 1982; 6: 655-663.
- [21] Fukatsu A, Tsuzuki T, Sassa N, Nishikimi T, Kimura T, Majima T, Yoshino Y, Hattori R and Gotoh M. Growth pattern, an important pathologic prognostic parameter for clear cell renal cell carcinoma. *Am J Clin Pathol* 2013; 140: 500-505.
- [22] Cornelis F, Tricaud E, Lasserre AS, Petitpierre F, Bernhard JC, Le Bras Y, Yacoub M, Bouzgarrou M, Ravaud A and Grenier N. Multiparametric magnetic resonance imaging for the differentiation of low and high grade clear cell renal carcinoma. *Eur Radiol* 2015; 25: 24-31.
- [23] Vargas HA, Delaney HG, Delappe EM, Wang Y, Zheng J, Moskowitz CS, Tan Y, Zhao B, Schwartz LH, Hricak H, Russo P and Akin O. Multiphasic contrast-enhanced MRI: single-slice versus volumetric quantification of tumor enhancement for the assessment of renal clear-cell carcinoma fuhrman grade. *J Magn Reson Imaging* 2013; 37: 1160-1167.
- [24] Lee HJ, Rha SY, Chung YE, Shim HS, Kim YJ, Hur J, Hong YJ and Choi BW. Tumor perfusion-related parameter of diffusion-weighted magnetic resonance imaging: correlation with histological microvessel density. *Magn Reson Med* 2014; 71: 1554-1558.
- [25] Lee EY, Hui ES, Chan KK, Tse KY, Kwong WK, Chang TY, Chan Q and Khong PL. Relationship between intravoxel incoherent motion diffusion-weighted MRI and dynamic contrast-enhanced MRI in tissue perfusion of cervical cancers. *J Magn Reson Imaging* 2015; 42: 454-459.
- [26] Dyvorne HA, Galea N, Nevers T, Fiel MI, Carpenter D, Wong E, Orton M, de Oliveira A, Feiweier T, Vachon ML, Babb JS and Taouli B. Diffusion-weighted imaging of the liver with multiple b values: effect of diffusion gradient polarity and breathing acquisition on image quality and intravoxel incoherent motion parameters—a pilot study. *Radiology* 2013; 266: 920-929.
- [27] Andreou A, Koh DM, Collins DJ, Blackledge M, Wallace T, Leach MO and Orton MR. Measurement reproducibility of perfusion fraction and pseudodiffusion coefficient derived by intravoxel incoherent motion diffusion-weighted MR imaging in normal liver and metastases. *Eur Radiol* 2013; 23: 428-434.
- [28] Kakite S, Dyvorne H, Besa C, Cooper N, Facciuto M, Donnerhack C and Taouli B. Hepatocellular carcinoma: short-term reproducibility of apparent diffusion coefficient and intravoxel incoherent motion parameters at 3.0T. *J Magn Reson Imaging* 2015; 41: 149-156.